

doi:10.15199/48.2021.04.27

## Advanced Control Strategy based on second order sliding mode of DFIG for Power System Fault Ride Through

**Abstract.** This study proposes a second order sliding-mode direct power control (SOSM-DPC) strategy for a grid-connected bidirectional power converter feeding a doubly fed induction generator (DFIG) with slip power recovery. New advanced control design, for the rotor and grid side converters of DFIG is adopted to enhance the fault ride-through (FRT) capability according to the grid connection requirement. Simulations performed under Matlab/Simulink authenticate the feasibility of the designed second order sliding mode -DPC. Simulation results on a 200VA DFIG system under normal and faulted grid voltage conditions demonstrate good performance of the proposed approach in terms of robustness and FRT capability.

**Streszczenie.** W artykule przedstawiono strategię bezpośredniego sterowania mocą (DPC) oraz strategię sterowania ślizgowego drugiego rzędu (SOSM), wykorzystane do sterowania dwukierunkowym przepływem mocy. Przekształtnik przyłączony jest do obwodu wirnika generatora indukcyjnego podwójnie zasilanego (DFIG). Te nowe zaawansowane strategie sterowania (SOSM-DPC) zostały zastosowane do przekształtnika wirnikowego i przekształtnika sieciowego generatora DFIG w celu zwiększenia wymaganej przepisami odporności układu na stany awaryjne i zakłócenia (FRT) występujące w sieci zasilającej. (Zaawansowana strategia sterowania ślizgowego drugiego rzędu generatorem DFIG)

**Keywords:** doubly fed induction generator (DFIG), sliding mode control, fault ride through, direct power control.

**Słowa kluczowe:** sterowanie ślizgowe, podwójnie zasilany generator indukcyjny (DFIG), funkcja usuwania usterek (FRT),..

### Introduction

The doubly fed induction generator (DFIG) presents many advantages over other types of generators. Among these, four quadrant active and reactive power capabilities and variable speed operation at low power loss are very interesting features for power generation in large wind turbine (WT). The typical topology of a DFIG based WT connected to the grid is shown on Fig. 1. In this configuration the stator of the generator is connected directly to the grid, to which it delivers most of its generated power. The rotor is connected to the grid by using back to back converters as Fig. 1 suggests. Depending on the rotor speed, the grid side converter (GSC) works in dual cooperation with the rotor side converter (RSC), permitting seamless energy flow in both directions. It also controls direct current (DC) bus voltage and adjust grid-side power factor, which makes the entire WT to have a flexible reactive power regulation [1].

An important issue raised by the recent increase in the penetration of the WT into the distribution networks is the fault ride through (FRT) capability [3]. Several grid codes prescribe for WT the requirement to stay connected to the grid during faults and voltage variations. Many approaches have been proposed in the literature to achieve the FRT, especially for the DFIG. The conventional rotor circuit crowbar is the most popular solution adopted in current industry to fulfill the FRT requirement [2]. During the fault, the RSC and GSC are disabled and a bypass resistor (the crowbar) is inserted in the rotor circuit, converting the DFIG to a simple induction generator. With an increased rotor resistance, the DFIG can still supply active power to the grid, but with a decreased electrical time constant that accelerates the energy dissipation and reduce the rotor transient current [3]. However, as longer the crowbar remains connected, higher the reactive power absorption arises, which can delay the grid voltage reconstruction after the fault is removed [4].

In [5], an FRT control strategy based on flux linkage tracking is designed for the RSC to limit the rotor current during grid faults. Hence, the rotor flux linkage is controlled by altering the output rotor voltage of the RSC in order to track as rapidly as possible the changing stator flux linkage.

In [6], a braking resistor is inserted on the DC-link. This resistor is switched on when a fault occurs, to smooth the

DC-link voltage during heavy imbalance of active power through the rotor-side and the grid-side converter.

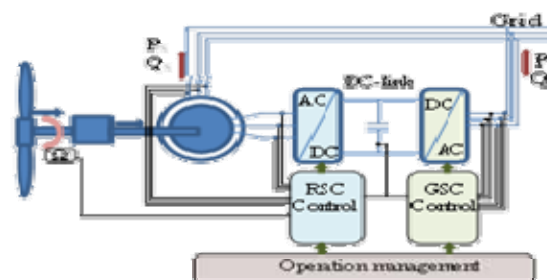


Fig.1. Configuration of DFIG

Some researchers have assumed that the crowbar was uneconomic and avoid the use of crowbar control. Instead, they developed a new power converter topology and fault control strategy. However, this makes the control system and coordination between normal and fault operation very complex. A combined protection and control strategy used to enhance the transient performance is given in [6]. Flexible AC transmission systems (FACTS) devices are proposed with shunt or series compensation topologies [7]. Nevertheless, these FACTS ensure only partial system protection. They are inadequate to prevent either rotor overcurrent or dc-link over voltage. To achieve full system protection, this scheme is usually combined with DC-link resistors and crowbar, which increase system complexity and cost [8].

In [9], authors present an innovative control strategy to enhance the FRT capacity of the DFIG without the need of additional current and voltage protections. During a grid fault, the generator rotor speed is increased through proper control of each converter. The key concept is to transform the unbalance energy into kinetic energy, instead of being dissipated otherwise. PI-based standard vector control is used for both converters control. However, the decoupling procedures involve feed-forward compensation, which is sensitive to the system parameters. Thus, the performance of vector control depends on the accuracy of system parameters [10].

In order to tackle the drawbacks highlighted earlier, this paper presents a direct power control (DPC) for both rotor and grid side converters of DFIGs, using a new control scheme based on a sliding mode approach (SMC).

Because of the unmodeled parts of the system and the non-ideal switching characteristic, conventional SMC create a chattering phenomenon (i.e. dangerous high-frequency vibrations), which limits its practical implementation [11]. Some terms of tracking error are introduced with equivalent control to mitigate the chattering effect as an integral function for example, or saturation function.

In this research, a control technique named super-twisting algorithm (STA) is adopted. It was introduced by Levant in 1993, and the name has been used since the publication of Bartolini [12]. Comparing with other second order sliding mode algorithm, the STA is characterized by having a bounded continuous control with discontinuities in the control derivative. In addition: 1) it does not require the time derivative information of the sliding variables, 2) when the system is of first-order relative degree, the STA can be applied directly and does not need to introduce new control variables [13][14]. Encouraging results have been obtained applying the STA to diverse configurations of electromechanical systems [12][14]. In this way, the proposed second order sliding mode-based STA combined with FRT strategy for DPC enables the DFIG to successfully comply with fault ride-through regulations stipulated by the grid codes.

### Direct power control of DFIG based on second order sliding mode control

Considering the supply grid and three-phase voltage source converter as ideal voltage sources, in Park reference frame, the DFIG voltage and flux equations are given by [15] and [16]. Adopting the motor convention, the  $P_s$  and  $Q_s$  (stator active and stator reactive powers) flowing between the stator of DFIG and the network can be expressed as

$$(1) \quad \frac{d}{dt} \begin{bmatrix} P_s \\ Q_s \end{bmatrix} = \begin{bmatrix} \frac{L_r}{\sigma M^2} R_s & -(\omega + \omega_s) \\ (\omega + \omega_s) & \frac{L_r}{\sigma M^2} R_s \end{bmatrix} \begin{bmatrix} P_s \\ Q_s \end{bmatrix} + \frac{\omega_r L_r}{\sigma M^2} \begin{bmatrix} V_{qs} & -V_{ds} \\ V_{ds} & V_{qs} \end{bmatrix} \begin{bmatrix} \phi_{ds} \\ \phi_{qs} \end{bmatrix} - \frac{R_r}{\sigma M} \begin{bmatrix} V_{ds} & V_{qs} \\ V_{qs} & -V_{ds} \end{bmatrix} \begin{bmatrix} i_{dr} \\ i_{qr} \end{bmatrix} - \frac{L_r}{\sigma M^2} \begin{bmatrix} V_{ds}^2 + V_{qs}^2 \\ 0 \end{bmatrix} + \frac{1}{\sigma M} \begin{bmatrix} V_{ds} & V_{qs} \\ V_{qs} & -V_{ds} \end{bmatrix} \begin{bmatrix} V_{dr} \\ V_{qr} \end{bmatrix}$$

In order to design the SMC Law, we describe the switching surface which depends on active and reactive power. The switching surface ensures that the  $P_s$  and  $Q_s$  track their references. In second step, we define the reaching law that will force the system to move towards the designed surface. Finally, we introduce additional term to alleviate the chattering effect on the switching surface.

The equivalent command corresponding to the ideal sliding regime is obtained as [15]

$$(2) \quad \begin{cases} \frac{dS_P}{dt} = \frac{d(P_s^* - P_s)}{dt} + K_{ps}(P_s^* - P_s) = -\frac{dP}{dt} + K_{ps}(P_s^* - P_s) \\ \frac{dS_Q}{dt} = \frac{d(Q_s^* - Q_s)}{dt} + K_{qs}(Q_s^* - Q_s) = -\frac{dQ}{dt} + K_{qs}(Q_s^* - Q_s) \end{cases}$$

The sliding surface can be written in the form:

$$(3) \quad \frac{dS}{dt} = F + DV_{rdq}$$

The rotor voltage can be calculated by imposing  $S = 0$ . In order to obtain good commutation around the surface and dynamic performances, the term  $k_{sgm} \text{Sgn}(S_p)$  was added to the equivalent control which will be expressed by [15]:

$$(4) \quad U_{ir} = \begin{bmatrix} U_{dr} \\ U_{qr} \end{bmatrix} = D^{-1} \begin{bmatrix} -\frac{dP}{dt} + K_{ps}(P_s^* - P_s) + K_{psgm} \text{Sgn}(S_p) \\ -\frac{dQ}{dt} + K_{qs}(Q_s^* - Q_s) + K_{qsgm} \text{Sgn}(S_Q) \end{bmatrix}$$

with

$$(5) \quad D^{-1} = \frac{-\sigma M}{(V_{ds}^2 + V_{qs}^2)} \begin{bmatrix} V_{ds} & V_{qs} \\ V_{qs} & -V_{ds} \end{bmatrix}$$

The idea of the second order sliding mode control techniques is to zero a function of the system's states, the sliding variable, and its first time derivative. Hence, its control structure is relatively simple and no-much information is needed, it has become the most widely used high order sliding mode control method [14]. There are several second order sliding mode algorithms, each of them with their own characteristics. In particular, the super-twisting algorithm (STA) has a quite simple law and allows synthesizing a continuous control with discontinuous time derivative (in contradiction to those of the sub-optimal algorithm). And it only requires measurements of surface  $s$ . We apply the STA, by adding the switching control terms  $U_{iST}$  to the equivalent control terms  $U_{ir}$  given by (4). The new law is then

$$(6) \quad U_{irF} = U_{iST} + U_{ir}$$

Where  $U_{iST}$  are the switching controls terms that make the system in any initial state reach the sliding manifold in finite time. While  $U_{ir}$  are the equivalent control terms, which allow the system to move along the sliding manifold under ideal conditions, and these terms can speed up the response of the system and reduce the steady-state errors. These equivalent control terms are derived by letting

$\dot{S}_P = \dot{S}_Q = 0$ . If we define the functions  $H_P$  and  $H_Q$  as follows [18]:

$$(7) \quad \begin{cases} H_P = -(\omega + \omega_s)Q + \frac{\omega_r L_r}{\sigma M^2} (V_{qs} \phi_{ds} - V_{ds} \phi_{qs}) \\ \quad - \frac{R_r}{\sigma M} (V_{ds} i_{dr} + V_{qs} i_{qr}) + \frac{1}{\sigma M} V_{qs} V_{qr} \\ \quad - \frac{L_r}{\sigma M^2} (V_{ds}^2 + V_{qs}^2) - P_{s\_ref} \\ H_Q = (\omega + \omega_s)P_s + \frac{\omega_r L_r}{\sigma M^2} (V_{ds} \phi_{ds} + V_{qs} \phi_{qs}) \\ \quad - \frac{R_r}{\sigma M} (V_{qs} i_{dr} - V_{ds} i_{qr}) + \frac{1}{\sigma M} V_{qs} V_{dr} - Q_{s\_ref} \end{cases}$$

Then we have the derivate of the errors:

$$(8) \quad \begin{cases} \dot{e}_P = \frac{d(P_s^* - P_s)}{dt} = \frac{1}{\sigma M} V_{ds} V_{dr} + H_P + \frac{L_r}{\sigma M^2} R_s P_s \\ \dot{e}_Q = \frac{d(Q_s^* - Q_s)}{dt} = \frac{L_r}{\sigma M^2} R_s Q_s + H_Q - \frac{1}{\sigma M} V_{ds} V_{qr} \end{cases}$$

The second derivate of the errors can be written as:

$$(9) \begin{cases} \dot{e}_p = -\frac{1}{\sigma M} V_{ds} \dot{V}_{dr} + \dot{H}_p + \frac{L_r}{\sigma M^2} R_s \dot{P}_s \\ \dot{e}_q = -\frac{1}{\sigma M} V_{ds} \dot{V}_{qr} + \dot{H}_q + \frac{L_r}{\sigma M^2} R_s \dot{Q}_s \end{cases}$$

In finite time based on the STA approach, the terms  $U_{iST}$  are calculated according to [17]

$$(10) \begin{cases} U_{PST} = -\lambda_p |e_p|^{0.5} \text{Sgn}(e_p) - \chi_p \int \text{Sng}(e_p) dt \\ U_{QST} = -\lambda_q |e_q|^{0.5} \text{Sgn}(e_q) - \chi_q \int \text{Sng}(e_q) dt \end{cases}$$

Of which only the bounds  $\Gamma_m, \Gamma_M$  and  $\Phi$  are known:

$$(11) \begin{cases} 0 < \Gamma_{mp} < \frac{1}{\sigma M} V_{ds} < \Gamma_{Mp}, \left| \dot{H}_p + \frac{L_r}{\sigma M^2} R_s \dot{P}_s \right| < \Phi_p \\ 0 < \Gamma_{mq} < \frac{1}{\sigma M} V_{qs} < \Gamma_{mQ}, \left| \dot{H}_q + \frac{L_r}{\sigma M^2} R_s \dot{Q}_s \right| < \Phi_q \end{cases}$$

The sufficient conditions for finite-time convergence [18] are

$$(12) \begin{cases} \lambda_p > \frac{\Phi_p}{\Gamma_{MP}}, \quad \chi_p^2 \geq \frac{4\Phi_p(\lambda_p + \Phi_p)}{\Gamma_{mP}^2(\lambda_p - \Phi_p)} \\ \lambda_q > \frac{\Phi_q}{\Gamma_{MQ}}, \quad \chi_q^2 \geq \frac{4\Phi_q(\lambda_q + \Phi_q)}{\Gamma_{mQ}^2(\lambda_q - \Phi_q)} \end{cases}$$

In practice, the parameters are never assigned according to inequalities. Usually, the real system is not exactly known, and the parameters estimations are much larger than the actual values. The right way is to adjust the controller parameters during computer simulations. The RSC global sliding-mode control is illustrated in detail in Fig. 2.

Similar to the RSC control law considered in this section, we designed the GSC control. More details of the second order sliding mode control of the GSC can be found at [19]. In addition, more details about the stability proof for the RSC control system and the guidelines for control parameter adjustment are given by [20]. The GSC global sliding-mode control is illustrated in Fig.3.

### The proposed FRT control strategy

Voltage sag, also referred as voltage dip, is a phenomenon that the grid voltage drops below the normal rms level (down to 0.1~0.9 p.u.) for a short duration (typically 0.5~30 cycles). It is a critical issue which can result in permanent damages.

Therefore, DFIG is expected to have reasonable FRT capability, which is to support the grid as well as to protect themselves from being damaged. Fig. 4 represents a typical FRT capability curve. In order to support the grid, DFIG must stay connected until the state (i.e. voltage - time) is placed below the solid line in the figure. Further details on FRT capability can be found in the literatures (various attempts on FRT capability including crowbar protection, GSC and RSC controllability).

In this paper, considering constant wind power (constant mechanical torque), when the grid voltage dips occur, the power flowing into the grid are imbalanced instantaneously, causing unbalanced power follows between the grid and rotor side converters accompanied with excessive currents in the rotor and stator circuits. Therefore, the proposed FRT control strategy will be triggered for the both converter GSC and RSC. When the DFIG is operating at the rated speed, the acceleration may rush the DFIG speed above its rated value due to the proposed control scheme during the fault.

The control scheme of the RSC against grid faults is illustrated in Fig. 2. Therefore, the new control strategy will not cause excessive mechanical stress to the whole system. In [19], the stator voltage is reduced to zero during the grid fault causing enormously high transient current values. However, the authors in [20] use the PI regulator in associated with the term describing the DC current  $i_{or} = P_r/U_{dc}$ . This will compensate the instantaneous rotor power in the control scheme.

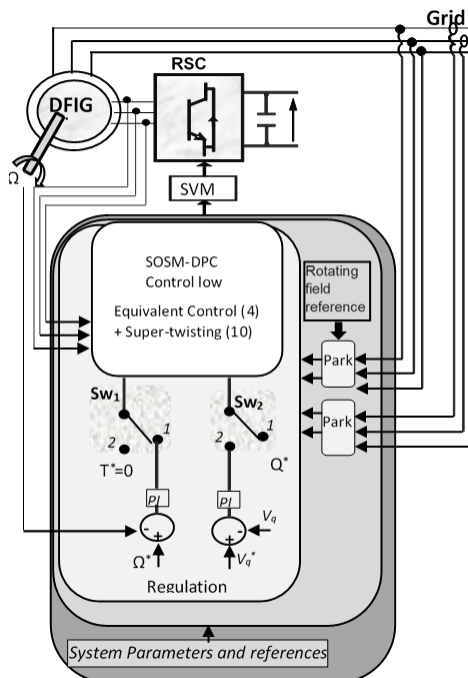


Fig.2. The RSC global second order sliding mode - DPC

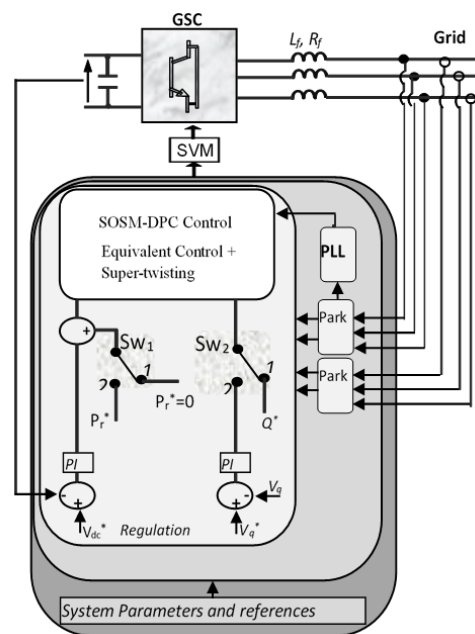


Fig.3. The GSC global second order sliding mode - DPC

In this paper we propose the detailed control scheme of the GSC during the grid fault in Fig. 3. The added term  $P_r^*$  is denoted as a disturbance to compensate the transient rotor power in the second order sliding mode control scheme. In such a way, the currents can be regulated smoothly during a grid fault. In Fig. 5, we present the global function of the DFIG control.

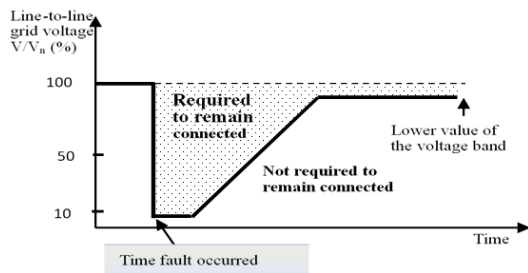


Fig.4. Typical low voltage ride through requirement

### Numerical explorations

Numerical studies have been performed on a 200-W, 208-V, 60-Hz wound-induction machine (using SimPowerSystems toolboxes with step time  $T=10e-5s$ ). The both systems of Fig. 2 and Fig. 3 were combined and have been simulated to verify the effectiveness of the proposed control method. Parameter data of the DFIG are shown in Table 1. At transient state, the WT dynamic hasn't high effect on the DFIG dynamic behaviour. The electrical system has high time constant compared with there of mechanical parameters of the turbine. Thus, we assume that the DFIG driven by constant mechanical torque. It's assumed a symmetrical three phase short circuit, in the grid with a reduced voltage of 20% to their nominal value. This fault appears between 0.3s and 0.37s. We think this strategy of control decrease the system transient behaviour. The stator reactive power is fixed by the control at 0VAR in all time of the simulation.

To better understand the functionality of the DFIG with back to back converters, we propose a fault scenario which can be described by the following sequence.

- 1) The simulation starts at  $t = 0$  s.
- 2) The system will reach the steady state at  $t = 2$  s.
- 3) A three-phase ground fault at the grid is applied occurs voltage sag of 20% dropped at  $t = 3$  s. for 500ms.
- 4) The protection and control switch as transient state operation at  $t=0.31$
- 5) The grid fault was cleared at  $t=3.5$
- 6) Coming back at normal grid operation at  $t=3.6s$

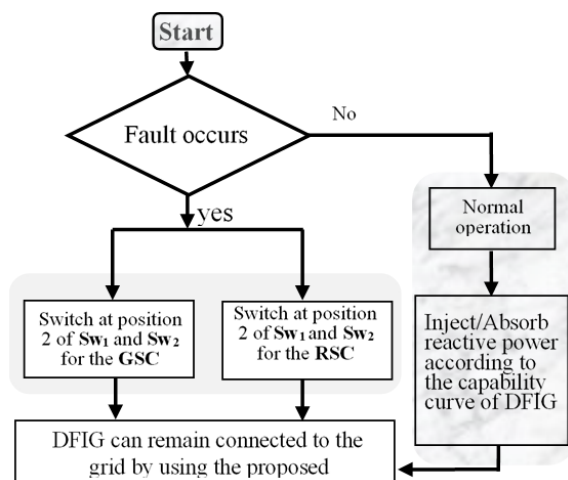
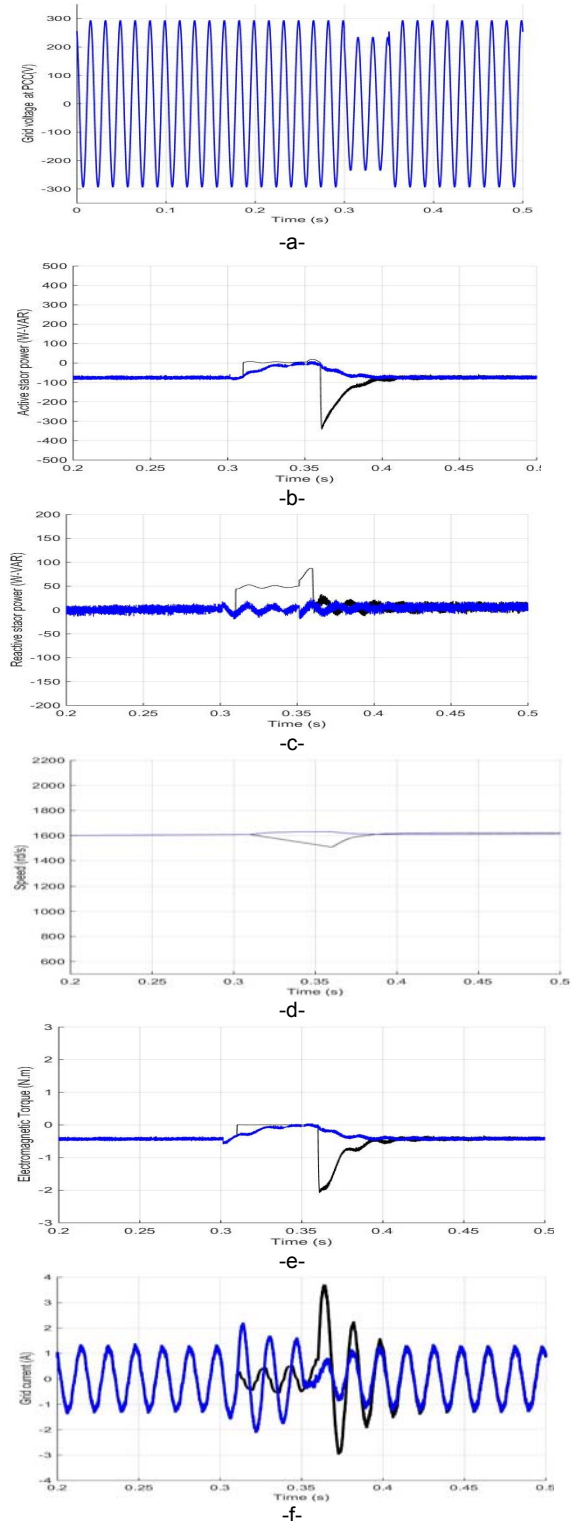


Fig.5. Proposed FRT for DFIG

We should precise that we have choose 0.1s time of the switch between two strategy control (at transient and steady state). With this short delay, avoid strength transient state at connexion and disconnection of the DFIG at the grid [15]. Furthermore, in the objective to demonstrate the robustness of the proposed control law, DFIG parameters where changed to have 10% variations (shown in Table 1). Under

these severe conditions two situations are performed for comparison studies: (A) conventional crowbar system utilized. (B) The proposed control strategy The FRT behaviours of the studied DFIG system operating at constant speed of 170rd/s, when the voltage at the PCC drops to 80% for 500 ms are shown in Fig. 6. During the fault, the rotor acceleration with the control strategy B is faster than the cases with the strategy A. This means that the additional energy can be transformed quickly into the kinetic one; therefore, the fluctuations of the torque, currents, and DC-link voltage are significantly reduced seen when employing crowbar methods.



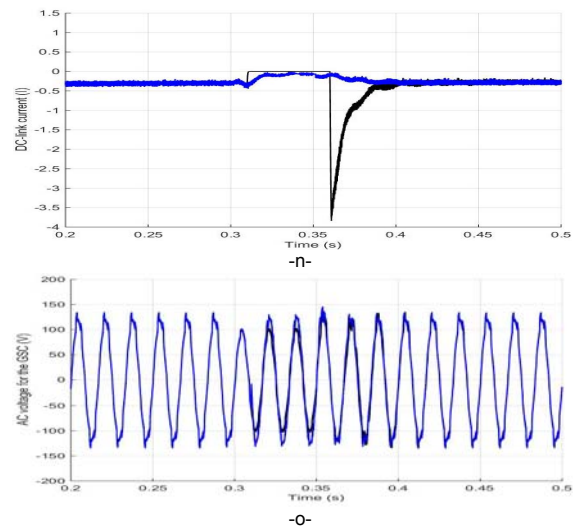
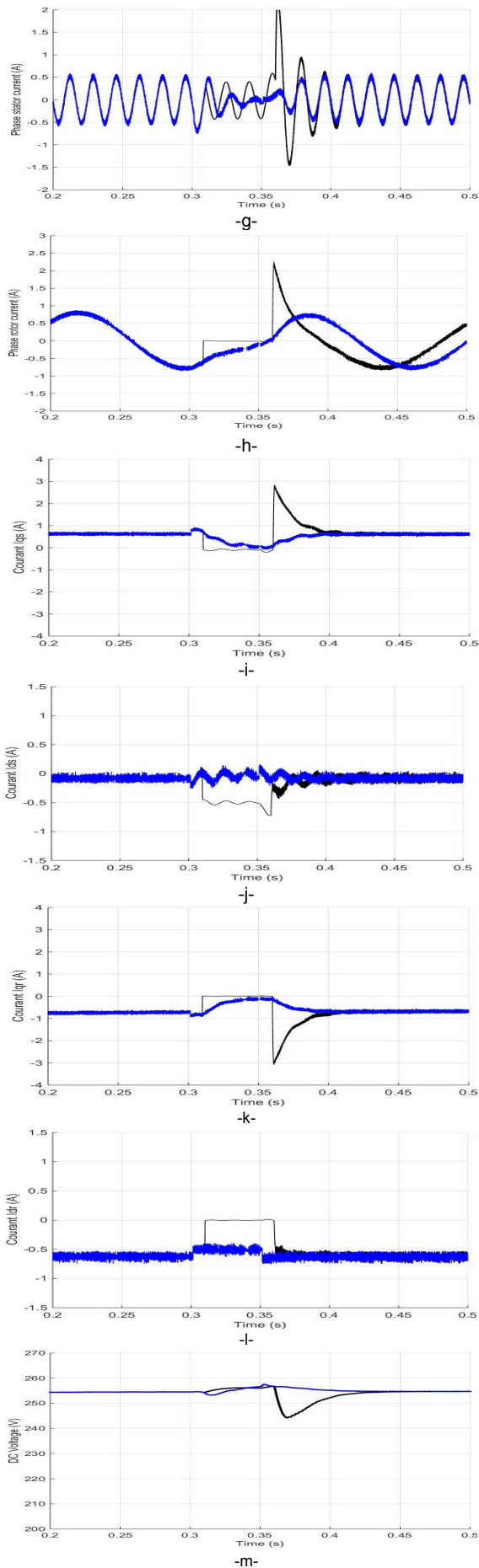


Fig.6. Simulated transient responses of the studied DFIG with the control strategies A (conventional crowbar) and B (newly proposed FRT based second order sliding mode strategy)

During the fault of the power system, the stator of DFIG will endure a large fault current because it is directly connected to the grid. The disturbance will be further transmitted to the rotor of DFIG. Hence, the rotor current will be very high, and this may lead to over current to the rotor side converter.

The in-fault stator voltage has been studied at 80% (Fig. 6a). Before fault clearance, the machine delivered 80W active power (Fig. 6b) and 0VAR reactive power (Fig. 6c). After fault clearance, the average value of reactive power falls from 80 import to zero over roughly 200 ms. At Fig. 6d the speed acceleration reaches 1600 rpm during fault. At the same time, the torque fell from 0.4 Nm import to 0 (Fig. 6e). The currents also reach 3.5A and 2.5A at the grid side (Fig. 6f) and the stator side (Fig. 6g) respectively. While the proposed control strategy B can suppress the transient values, which is below the activation threshold of the crowbar.

The GSC also switched to reactive current control mode during fault condition. After fault initiation, the rotor currents (Fig. 6h) showed speed oscillations and clearance reflecting the near-dc decay on the stator circuit.

During the grid fault condition, the RSC control is switched to supply reactive current by giving priority to. To illustrate the effectiveness of reactive current control mode precisely, the active and reactive components of the stator and rotor currents during fault are depicted in Fig. 6i, Fig. 6j, Fig. 6k and Fig. 6l. To track these reference currents, the RSC injects an average rotor voltage, across the rotor terminals which force the rotor current, to flow in rotor winding and corresponding stator current, in stator winding.

Fig.6m shows that with the strategy A, the fluctuation of the DC-link voltage is not damped sufficiently compared with the strategy B. same behavior at Fig.6n. the DC-link current has been effectively reduced.

Fig. 6o presents the grid side voltage. This demonstrates the GSC converter contribution to improve the voltage wave. Hence, the voltage kept his permanent value as shown in Fig. 6p. Consequently, it is observed that after the fault clearance, the rotor speed decreases back to the reference value and the oscillations are well damped under the proposed control. Especially, this approach can suppress the transient currents lower than the crowbar threshold.

Accordingly, the proposed control strategy can allow the DFIG to ride through this fault even without activating the conventional crowbar protection.

## Conclusion

This paper dealt with second order sliding mode control of doubly-fed induction generator –DFIG- based wind turbines –WTs-. Simulations results on a 200w grid-connected DFIG (under normal and faulted grid voltage conditions) clearly show the second order sliding mode control based direct power control -DPC- scheme efficiency and attractiveness in terms of finite reaching time, chattering-free behavior, robustness with respect to external disturbances and fault ride through –FRT- capability enhancement.

Grid fault-tolerance has been investigated using second order sliding mode control for both converters' generator and grid side converter. The new approach introduces a compensation item to the grid side controller in order to suppress the DC-link over-voltage during the faults. Compared with conventional crowbar technique, the new control strategy enables the DFIG to continue the electricity production and absorb the excessive energy by increasing the generator rotor speed temporarily when a grid fault occurs.

The test results indicate the FRT-based second order sliding mode is a potentially useful to protect power converters and improve the FRT capability of the DFIG-WT. The sought solution is purely software-based as it is achieved through the adjustment of the both converters control without the requirement of additional devices such as crowbars, voltage restorers, etc. Thus, the achievable benefits are the enhancement in fulfilling grid code requirements, and the reduction of costly devices that take up space, add weight and increase DFIG-WT maintenance costs.

## Annex

Table 1. Parameters of DFIG

Parameter	Value
Nominal power	200W
Stator voltage / frequency	110V/60Hz
Number of pole pairs	2
Stator Resistance, $R_s$	12.5 $\Omega$
Stator leakage inductance, $L_s$	0.5 H
Magnetizing inductance, $M$	0.47H
Rotor Resistance, $R_r$	3.9 $\Omega$
Rotor leakage inductance, $L_r$	0.5 H
DC-link rated voltage, $V_{dc}$	200V
DC-link capacitance, $C_{dc}$	1400 $\mu$ F
Grid-side line inductance, $L_f$	0.04H
Grid-side line resistance, $R_f$	0.1 $\Omega$

### Authors:

Djilali kairous

Faulty of technologie.

Université of Hassiba Benbouali at Chlef - BP 78C , Ouled Fares, Chlef 02180. Chlef. Algeria.

E-mail: [d.kairous@univ-chlef.dz](mailto:d.kairous@univ-chlef.dz)

Mustapha BENGHANEM

Faulty of electrical en generiing.

Université of Sciences and Technology at Oran - BP 1505, Bir El Djir, Oran 31000. Algeria.

E-mail: [mbenghanem69@yahoo.fr](mailto:mbenghanem69@yahoo.fr)

## REFERENCES

- [1] Yaramasu V., Wu B., Sen P.C., Kouro S., High-Power Wind Energy Conversion Systems: State-of-the-Art and Emerging Technology, *Proceedings of the IEEE*, Vol: 103, Issue: 5, pp. 740 – 788. 2015.
- [2] Cheng M., Cai X., Wu G., Investigation of Transient Torque during a Power System Fault in Wind Power Turbines Having a DFIG and Crowbar Circuit, *Przeegląd Elektrotechniczny*, 11a/2010, 43-47.pg.245
- [3] Mokryani G., Siano P., Piccolo A., Chen Z., Improving fault ride through capability of variable speed wind turbines in distribution networks, *IEEE Sys. Journal.*, In Press.2013.
- [4] Kairous D., Wamkeue R., Belmadani B., Benghanem M., Dynamic performances and protection scheme for Doubly-fed Induction Generator during disturbances, *IEEE-EPEC*, Ohrid 6-8 Sept. 2010.
- [5] Xiao S., Yang G., Zhou H., Geng H., An LVRT control strategy based on flux linkage tracking for DFIG-based WECS, *IEEE Trans. Ind. Electron.*, vol. 60, no. 7, pp. 2820-2832, July. 2013.
- [6] Tsili M., Papathanassiou S., A review of grid code technical requirements for wind farms," *IET Renew. Power Gener.*, vol. 3, no.3, pp.308–332,2009.
- [7] Ambati B.B., Kanjiya, P., Khadkikar V., A low Component Count Series Voltage Compensation Scheme for DFIG WTs to Enhance Fault Ride-Through Capability, *IEEE Transactions on Energy Conversion*, Vol. 30, No. 1, March 2015
- [8] Huang P., El Moursi M.S., Hasen S.A., Novel Fault Ride-Through Scheme and Control Strategy for Doubly Fed Induction Generator-Based Wind Turbine, *IEEE Transactions on Energy Conversion*, Vol. 30, NO. 2, JUNE 2015.
- [9] Yang, L., Xu Z., Østergaard, J. – Dong, Z.Y – Wong, K.: Advanced Control Strategy of DFIG Wind Turbines for Power System Fault Ride Through, *IEEE Transactions on Power Systems*, Vol. 27, No. 2, Pp.713-722. 2012.
- [10] Pena R., Clare J. C., Asher G.M.: Doubly fed induction generator using back-to-back PWM converters and its application to variable-speed wind-energy generation, *IEE Proceedings-Electric PowerApplications*, 143(3), pp. 231-241, 1996.
- [11] Laghrouche S., Robust second order sliding mode control for a permanent magnet synchronous motor, *American Control Conference*, pp.4071-4076, (2003).
- [12] Zhu X., Liu S., Wang Y., Higher Control Scheme Using Neural Second Order Sliding Mode and ANFIS-SVM strategy for a DFIG-Based Wind Turbine, *3rd Renewable Power Generation Conference*, Naples, 24-25 Sept. 2014, pp. 1-6.
- [13] Zheng X., Li W., Wang W., High-order sliding mode controller for no-load cutting-in control in dfig wind power system, *Systems and Control in Aeronautics and Astronautics (ISCAA), 2010 3rd International Symposium on*, 2010.
- [14] Kairous D., Wamkeue R., Belmadani B., Benghanem M., Robust SMC for SV-PWM based indirect power control of DFIG, *Przeegląd Elektrotechniczny*, 11a/2010, 43-47.
- [15] Kairous D., Wamkeue R., Sliding-mode control approach for direct power control of WECS based DFIG, *EEEIC*, Italy, 8-11 May 2011. Pp. 1-4, 2011.
- [16] Krause P.C., Wasynczuk O., Sudhoff, S.D., Analysis of Electric Machinery and Drive Systems, *IEEE Press*, 2nd ed. 2000.
- [17] Fridman L., Levant A., Higher-order sliding modes, Chap 3, in Sliding mode control in engineering, *Eds. Marcel Dekker*, 2002, pp. 53–101, isbn 0-8247-0671-4.
- [18] Kairous D., Beaudoin J.J., Wamkeue R., Ouhrouche, M., Sliding mode control for voltage source converter applied to wind energy systems, *ICRERA*, Milwaukee, USA, pp. 289 – 294. 2014.
- [19] Martinez M.I., Tapia G., Susperregui A., Camblong, H.: Sliding-Mode Control for DFIG Rotor- and Grid-Side Converters Under Unbalanced and Harmonically Distorted Grid Voltage, *IEEE Transactions on Energy Onversion*, Vol. 27, No. 2, June 2012.
- [20] Yao J., Li H., Liao Y., Chen, Z., An improved control strategy oflimiting the DC-link voltage fluctuation for a doubly fed induction wind generator, *IEEE Trans. Power Electron.*, vol. 23, no. 3, pp. 1205–1213, May 2008.